

A FAST AND EFFICIENT CHANGE-POINT DETECTION FRAMEWORK FOR MODERN DATA

BY YI-WEI LIU AND HAO CHEN

University of California, Davis

Change-point analysis is thriving in this big data era to address problems arising in many fields where massive data sequences are collected to study complicated phenomena over time. It plays an important role in processing these data by segmenting a long sequence into homogeneous parts for follow-up studies. The task requires the method to be able to process large datasets quickly and to deal with various types of changes for high-dimensional and non-Euclidean data. We propose a novel approach making use of approximate k -nearest neighbor information of the observations, and derive an analytic formula to control the type I error. The time complexity of the method is $O(dn \log n)$ for an n -length sequence of d -dimensional data. Moreover, we incorporate a useful pattern of data in high dimension that the proposed method could detect various types of changes in the sequence.

1. Introduction. With advances in technologies, scientists in many fields are collecting massive data for studying complex phenomena over time and/or space. Such data often involve sequences of high-dimensional or non-Euclidean measurements that cannot be analyzed through traditional approaches. Insights on such data often come from segmentation/change-point analysis, which divides the sequence into homogeneous temporal or spatial segments. They are crucial early steps in understanding the data and in detecting anomalous events. Change-point analysis has been extensively studied for univariate data (see [Carlstein, Müller and Siegmund \(1994\)](#); [Chen and Gupta \(2011\)](#) for a review). However, methods for multivariate data are limited in many ways ([Chan et al., 2015](#); [Heard et al., 2010](#); [James, James and Siegmund, 1992](#); [Siegmund, Yakir and Zhang, 2011](#); [Srivastava and Worsley, 1986](#); [Wang et al., 2013](#); [Wang and Samworth, 2018](#); [Xie and Siegmund, 2013](#); [Zhang et al., 2010](#)), and there is little research for non-Euclidean data ([Chen and Zhang, 2015](#); [Chu and Chen, 2019](#); [Harchaoui, Moulines and Bach, 2009](#); [Matteson and James, 2014](#)). Many modern applications require effective and fast change-point detection for high-dimensional/non-Euclidean data. The follows are some examples.

Network evolution: Network data have become increasingly popular. For example, phone calls, emails, or online chat records can be used to construct networks depicting social interactions among individuals ([Eagle, Pentland and Lazer, 2009](#); [Kossinets and Watts, 2006](#)). In biological science, the study of gene-interaction network is omnipresent ([Li et al., 2011](#); [Lu et al., 2011](#)). A crucial part of these studies is identifying how the networks evolve in time. For the above examples, the observations at each time point is a graphical encoding of the underlying network. Researchers might be interested in asking whether there is a change in network structure over time.

Public transportation demand analysis: The study of public goods allocation is drawing attention as tons of data on public activities can be collected easily nowadays, such as the NYC taxi and limousine commission data (<https://www1.nyc.gov/site/tlc/about/tlc-trip-record-data.page>). Take transportation as an example, studies are performed to better meet the supply with aggregate demand. Such intension can be achieved by characterizing whether the public demands for certain transportation are distinct in different time intervals. Here, the observation at each time point could be a heatmap illustrating the volume associated with pick-ups and drop-offs locations.

Neuropixels data processing: As the development of Neuropixels probes enlightens the field of neuroscience, the challenges in analyzing such large-scale and high-density data couldn't be over-emphasized. Neuropixels data usually consists of hundreds or thousands of long stretches of neuron spiking activities simultaneously (Chen, Chen and Deng, 2019). Scientists and researchers are striving to extract meaningful information from Neuropixels recordings (Stringer et al., 2019). It is of scientific interest to detect points in time at which population spiking activity exhibits simultaneous changes as well as changes that only occur in a subset of the neural population.

In the above examples, the observation can be a network, an image, or a long vector. Let the sequence of observations be $\{\mathbf{y}_t : t = 1, \dots, n\}$, indexed by some meaningful order, such as time or location. Then the change-point detection can be formulated as testing the null hypothesis of homogeneity:

$$H_0 : \mathbf{y}_t \sim F_0, t = 1, \dots, n, \quad (1)$$

against the alternative that there exists a change-point τ :

$$H_1 : \exists 1 \leq \tau < n, \mathbf{y}_t \sim \begin{cases} F_0, & t \leq \tau \\ F_1, & \text{otherwise,} \end{cases} \quad (2)$$

Here, F_0 and F_1 are two different probability measures. In practice, we usually do not know what F_0 and F_1 are, or what distributional family they belong to. This makes the parametric methods proposed for high-dimensional data not applicable.

Some non-parametric methods have been proposed, and there are mainly three categories:

1. Kernel-based method (Harchaoui, Moulines and Bach, 2009)
2. Distance-based method (Matteson and James, 2014)
3. Graph-based method (Chen and Zhang, 2015; Chu and Chen, 2019)

The kernel-based method depends on the choice of kernel and suffers from increased dimension. In addition, due to the nature of the kernel methods, there is currently no effective way of controlling the type I error under the change-point setting. It's extremely time consuming to apply the method when one would like to control the type I error. This makes the method not practically useful. The distance-based method was proposed in (Matteson and James, 2014). The authors use all the pairwise distances among observations to find change-points. Computing all

pairwise distances needs $O(dn^2)$ time for d -dimensional data. Moreover, there is no analytic formula to control type I error, so it's time consuming to run the method with proper type I error control (see Table 1). On the other hand, graph-based methods (Chen and Zhang, 2015; Chu and Chen, 2019) provide analytic formulas to control the type I error and are much faster to run.

Existing graph-based methods utilize an undirected graph constructed among observations. Some common choices are the minimum spanning tree (MST), where all observations are connected with the total distance minimized, the minimum distance pairing (MDP), where the observations are partitioned into $n/2$ pairs with the total within-pair distance minimized, the undirected nearest neighbor (NN) graph, where each observation connects to its nearest neighbor, and their denser versions, k -MST, k -MDP, and undirected k -NN graphs. Take the k -MST for example, it is the union of the 1st, \dots , k th MSTs, where the 1st MST is the MST, and the j th MST is a spanning tree connecting all observations such that the sum of the edges in the tree is minimized under the constraint that it does not contain any edge in the 1st, \dots , $(j-1)$ th MSTs. Among these graphs, k -MST is preferred as it in general has a higher power than others (Chen and Zhang, 2015). Nevertheless, it could take long to construct the k -MST when n is large. In this work, we propose a new statistic on a directed approximate k -NN graph. As the directed k -NN contains more useful information than the undirected k -NN graph, we find the new method having power on par with the existing method on k -MST. There are multiple existing algorithms to construct the directed approximate k -NN graph, and the computational cost can easily be achieved at $O(dn \log n)$. As the directed graph cannot be handled by the existing graph-based framework, we work out a new framework to handle them. In particular, we work out the limiting distribution of the new statistic and derive an analytic formula to control the type I error so that the time complexity of the method after the directed approximate k -NN graph is obtained is $O(n)$. Thus, the overall time complexity of the new method is the same as that for obtaining the approximate k -NN graph.

2. Main results. First, we compare the computational cost of our method to the other three state-of-the-art methods: graph-based method with the max-type statistic on 5-MST (the recommended setting in (Chu and Chen, 2019)), the distance-based method (ecp) (Matteson and James, 2014), and the kernel-based method (Harchaoui, Moulines and Bach, 2009). For our method, we use the k - d tree algorithm (Beygelzimer et al., 2019) to approximate the directed 5-NN graph. We use the 5-NN graph as it contains a similar number of edges to the 5-MST to make the comparison with the existing graph-based method fair. The observations are generated i.i.d. from a multivariate t_5 -distribution with dimension $d = 100$. The results are presented in Table 1. We also check the empirical size of these methods (Table 2). From these tables, we can see that the kernel-based method is slow to run and cannot control the type I error. The other three methods can control the type I error well. The graph-based methods are much faster than ecp, and the new method is more than 2-fold faster than the existing graph-based method on 5-MST for $n = 2,000$ or above.

Next, we compare the power of the three methods that could control the type

TABLE 1

Time comparison: Average time cost (\pm standard deviation) from 10 simulation runs for each choice of n . The environment where the experiments are conducted: CPU: Intel(R) Xeon(R) CPU E5-2690 0 @ 2.90GHz / RAM: DDR3 @ 1600MHz / OS: Scientific Linux 6.10 / 2.6.32 Linux.

n	1,000	2,000	5,000	10,000	20,000	30,000
New	1.9 (± 0.4)	3.5 (± 0.8)	11 (± 3.2)	47 (± 7.0)	227 (± 39)	478 (± 65)
5-MST	1.7 (± 1.0)	8.7 (± 4.6)	29 (± 8.9)	122 (± 27)	610 (± 144)	1,228 (± 212)
ecp	10.4 (± 5.8)	54 (± 14)	362 (± 108)	1,023 (± 228)	6,836 (± 214)	>10,000
kernel	548 (± 9.1)	9,153 (± 101)	>10,000	-	-	-

TABLE 2

Empirical size: Fractions of simulation runs (out of 10,000 simulations) that the null hypothesis is rejected at level α when there is no change-point in the sequence ($n = 1,000$).

	$\alpha = 0.10$	$\alpha = 0.05$	$\alpha = 0.01$
New	0.100	0.051	0.012
5-MST	0.097	0.052	0.013
ecp	0.101	0.054	0.011
kernel	1.000	1.000	1.000

I error. The length of the sequence is set to be $n = 1,000$ with a change-point happens at a quarter of the sequence, $\tau = 250$, for all simulations. We compare the power under four different scenarios. The specific amount of changes were chosen so that the tests are of moderate power to be comparable. We see that the new test is the most powerful or on par with the most powerful test over various types of changes. More simulations are provided in the supplement.

Scenario 1: The observations are generated from a d -dimensional multivariate Gaussian distribution with mean zero and covariance matrix Σ , where $\Sigma_{ii} \stackrel{\text{i.i.d.}}{\sim} U(1, 2)$, and $\Sigma_{ij} = ((h+1)^{2H} + (h-1)^{2H} - 2h^{2H})/2$, with $h = |i-j|$ and $H = 0.85$. After the change, all elements in the mean vector shift by 0.02, and the covariance matrix becomes $a\Sigma$. We use Δ to denote the mean vector and $\|\Delta\|_2$ to denote its L^2 norm after the change.

Scenario 2: The observations are generated from d -dimensional multivariate t_5 with mean zero, and the same covariance matrix as Scenario 1. After the change, all elements in the mean vector Δ shift by the same amount, and the covariance matrix becomes $a\Sigma$.

Scenario 3: The observations are generated from d -dimensional multivariate t_5 with mean zero, and covariance matrix Σ with $\Sigma_{ij} = 0.6^{|i-j|}$. After the change, the covariance matrix becomes $\Sigma_{ij} = \rho^{|i-j|}$. Note that here only the off-diagonal elements of Σ change.

Scenario 4: The observations are generated from d -dimensional independent exponential distributions with scale parameter 1. After the change, all the d scale parameters become λ .

TABLE 3

Power comparison: *Fractions of times (out of 100) the null hypothesis is rejected under $\alpha = 0.05$ for various data dimensions and sizes of chnage.*

Scenario 1						Scenario 2					
d	25	100	500	1000	2000	d	25	100	500	1000	2000
$\ \Delta\ _2$	0.10	0.20	0.45	0.63	0.89	$\ \Delta\ _2$	0.25	0.50	1.12	1.58	2.24
a	1.10	1.06	1.03	1.02	1.02	a	1.25	1.27	1.30	1.32	1.32
New	0.73	0.84	0.83	0.73	0.93	New	0.85	0.83	0.74	0.77	0.83
5-MST	0.68	0.82	0.80	0.72	0.92	5-MST	0.84	0.82	0.79	0.82	0.86
ecp	0.08	0.06	0.05	0.10	0.05	ecp	0.07	0.35	0.55	0.87	0.89

Scenario 3						Scenario 4					
d	25	100	500	1000	2000	d	25	100	500	1000	2000
ρ	0.50	0.40	0.35	0.30	0.15	λ	1.10	1.05	1.03	1.02	1.02
New	0.75	0.76	0.63	0.58	0.60	New	0.81	0.67	0.70	0.61	0.87
5-MST	0.63	0.79	0.65	0.63	0.64	5-MST	0.78	0.66	0.73	0.69	0.91
ecp	0.06	0.07	0.06	0.03	0.05	ecp	0.92	0.67	0.56	0.30	0.47

3. New statistic. Given a **directed** similarity graph $G = \{(i, j) : \mathbf{y}_i \text{ points to } \mathbf{y}_j\}$, let $R_{G,1}(t)$ be the number of edges on G connecting both observations before t , and $R_{G,2}(t)$ be the number of edges on G connecting both observations after t :

$$R_{G,1}(t) = \sum_{(i,j) \in G} \mathbb{1}_{\{i \leq t, j \leq t\}} \quad \text{and} \quad R_{G,2}(t) = \sum_{(i,j) \in G} \mathbb{1}_{\{i > t, j > t\}},$$

with $\mathbb{1}_A$ the indicator function for event A . Figure 1 illustrates the computation of $R_{G,1}(t)$ and $R_{G,2}(t)$ on a toy example. For the directed approximate k -NN graph, each observation points to k other observations. Similar to the undirected graph version in (Chen and Zhang, 2015) and (Chu and Chen, 2019), we can define four edge-count scan statistics (original/weighted/generalized/max-type) for directed graphs. Here, we focus on the max-type edge-count scan statistic and leave the other three to the supplement.

Since our method is non-parametric, we work under the permutation null distribution that places $1/n!$ probability on each of the $n!$ permutations of $\{\mathbf{y}_i : i = 1, \dots, n\}$. With no further specification, we use \mathbf{P} , \mathbf{E} , \mathbf{Var} , and \mathbf{Cov} to denote probability, expectation, variance, and covariance, respectively, under the permutation null distribution. For each candidate t of the true change-point τ , the max-type edge-count test statistic is defined as

$$M(t) = \max(Z_w(t), |Z_{\text{diff}}(t)|), \quad (3)$$

where

$$Z_w(t) = \frac{R_w(t) - \mathbf{E}(R_w(t))}{\sqrt{\mathbf{Var}(R_w(t))}} \quad \text{and} \quad Z_{\text{diff}}(t) = \frac{R_{\text{diff}}(t) - \mathbf{E}(R_{\text{diff}}(t))}{\sqrt{\mathbf{Var}(R_{\text{diff}}(t))}},$$

with $R_w(t) = \frac{n-t-1}{n-2} R_{G,1}(t) + \frac{t-1}{n-2} R_{G,2}(t)$ and $R_{\text{diff}}(t) = R_{G,1}(t) - R_{G,2}(t)$. The null hypothesis of homogeneity is rejected if the scan statistic

$$\max_{n_0 \leq t \leq n_1} M(t) \quad (4)$$

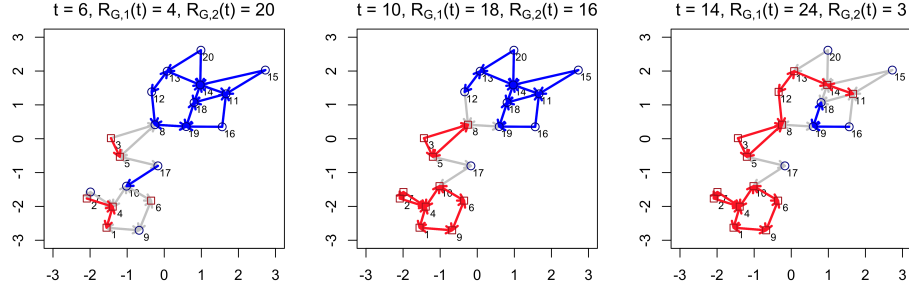


FIG 1. The computation of $R_{G,1}(t)$ and $R_{G,2}(t)$ at three different values of t . The first 10 observations are drawn from $N((-0.5, -0.5)^T, \mathbf{I}_2)$, and the second 10 observations are drawn from $N((0.5, 0.5)^T, \mathbf{I}_2)$, where \mathbf{I}_2 is the 2×2 identity matrix. Here, G is the directed 2-NN on Euclidean distance. Each t divides the observations into two groups: one group for observations before t (squares) and the other group for observations after t (circles). Red edges connect observations before t and the count is $R_{G,1}(t)$; blue edges connect observations after t and the count is $R_{G,2}(t)$. Notice that as t changes, the group identities change but the graph G does not change.

with n_0 and n_1 pre-specified, is larger than the critical value for a given significance level.

From the definition of $M(t)$, we see that either a large value of $Z_w(t)$ or $|Z_{\text{diff}}(t)|$ would contribute to the scan statistic. They corresponds to two major exhibitions of the graph when there is a change at t . When $\{\mathbf{y}_1, \dots, \mathbf{y}_t\}$ and $\{\mathbf{y}_{t+1}, \dots, \mathbf{y}_n\}$ are from the same distribution, they are well mixed and $R_{G,1}(t)$ and $R_{G,2}(t)$ would be close to their null expectations (Figure 2 (a)). When they are from different distributions, one common exhibition is that observations from the same distribution are more likely to be connected in G . Figure 2 (b) plots a typical directed 2-NN graph under this alternative and we see there are very few edges connecting between the two groups. When this happens, $Z_w(t)$ is large. For moderate- to high- dimensional data, another exhibition of the graph is common under alternative shown in Figure 2 (c). We see that $R_{G,1}(t)$ is much larger than its null expectation but $R_{G,2}(t)$ is much smaller than its null expectation (very few blue edges). This happens due to **the curse of dimensionality**. Here, the dimension is $d = 100$. The circles are from a distribution with a larger variance than those of the squares. As the volume of a d -dimensional ball increases exponential in d , circles are sparsely scattered and tend to find their nearest neighbors in squares. The $Z_{\text{diff}}(t)$ part in our statistic is effective in capturing this pattern. The absolute value is to cover the two possible scenarios in opposite directions showcased in Figure 2 (c) and (d).

THEOREM 1. *The expectation, variance and covariance of $R_{G,1}(t)$ and $R_{G,2}(t)$ on the directed approximate k -NN graph G are:*

$$\begin{aligned} E(R_{G,1}(t)) &= nkp_1(t), \quad E(R_{G,2}(t)) = nkq_1(t), \\ \text{Var}(R_{G,1}(t)) &= \left(c^{(1)} + c^{(2)}\right)p_1(t) + \left(c^{(3)} + c^{(4)} + c^{(5)} + c^{(6)}\right)p_2(t) + c^{(7)}p_3(t) - (nkp_1(t))^2, \\ \text{Var}(R_{G,2}(t)) &= \left(c^{(1)} + c^{(2)}\right)q_1(t) + \left(c^{(3)} + c^{(4)} + c^{(5)} + c^{(6)}\right)q_2(t) + c^{(7)}q_3(t) - (nkq_1(t))^2, \end{aligned}$$

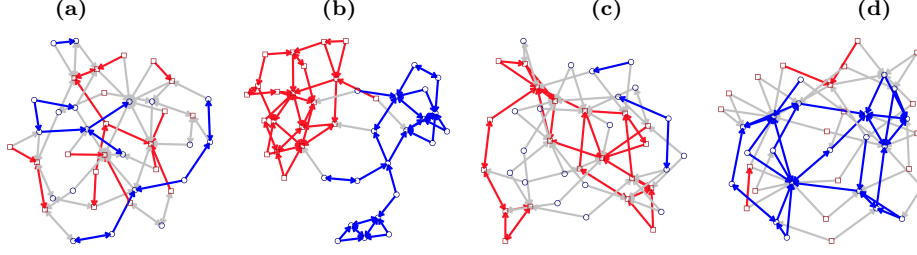


FIG 2. Directed 2-NN graphs on 100-dimensional data visualized by the `ggnet2` function. Here, $\mathbf{y}_1, \dots, \mathbf{y}_{20}$ (squares) are drawn from the standard 100-dimensional Gaussian distribution, and $\mathbf{y}_{21}, \dots, \mathbf{y}_{40}$ (circles) are drawn from $N_{100}(\mu, a\mathbf{I}_{100})$ with (a) $\mu = \mathbf{0}, a = 1$; (b) $\mu = 0.8\mathbf{1}, a = 1$; (c) $\mu = \mathbf{0}, a = 1.4$; (d) $\mu = \mathbf{0}, a = 0.8$. Same edge coloring scheme as in Figure 1.

$$\text{Cov}(R_{G,1}(t), R_{G,2}(t)) = c^{(7)}r(t) - (nk p_1(t))(nk q_1(t)),$$

with

$$\begin{aligned} p_1(t) &= \frac{t(t-1)}{n(n-1)}, & p_2(t) &= \frac{t(t-1)(t-2)}{n(n-1)(n-2)}, & p_3(t) &= \frac{t(t-1)(t-2)(t-3)}{n(n-1)(n-2)(n-3)}, \\ q_1(t) &= \frac{(n-t)(n-t-1)}{n(n-1)}, & q_2(t) &= \frac{(n-t)(n-t-1)(n-t-2)}{n(n-1)(n-2)}, \\ q_3(t) &= \frac{(n-t)(n-t-1)(n-t-2)(n-t-3)}{n(n-1)(n-2)(n-3)}, & r(t) &= \frac{t(t-1)(n-t)(n-t-1)}{n(n-1)(n-2)(n-3)}, \end{aligned}$$

where $c^{(1)}, \dots, c^{(7)}$ are quantities on the graph G , defined as:

$$\begin{aligned} c^{(1)} &= nk, & c^{(2)} &= \sum_{i=1}^n \sum_{j \in D_i} \mathbb{1}_{\{(i,j) \in G\}}, & c^{(3)} &= c^{(4)} = \sum_{i=1}^n \sum_{j \in D_i} (k - \mathbb{1}_{\{(i,j) \in G\}}), \\ c^{(5)} &= nk(k-1), & c^{(6)} &= \sum_{i=1}^n (|D_i|^2 - |D_i|), & c^{(7)} &= (nk)^2 - \sum_{m=1}^6 c^{(m)}. \end{aligned}$$

Here, D_i is the set of indices of observations that point toward observation \mathbf{y}_i , and $|D_i|$ is the cardinality of set D_i , or the in-degree of observation \mathbf{y}_i .

Theorem 1 can be proved by combinatorial analysis. The expectations are relatively simple due to the linearity of expectation. For the variances and the covariance, we have to figure out the number of possible configurations of pairs of edges plotted in Figure 3. A detailed proof of the theorem is in the supplement.

Next, we show when the max-type edge-count scan statistic $M(t)$ in (3) is well-defined in Theorem 2, and its proof is in the supplement.

THEOREM 2. *The max-type edge-count scan statistic $\{M(t)\}_{t=1, \dots, n-1}$ on an approximate k -NN graph is well-defined when $n \geq 5$ and not every observation has the same in-degree (i.e., there exists an i , $1 \leq i \leq n$, such that $|D_i| \neq k$).*

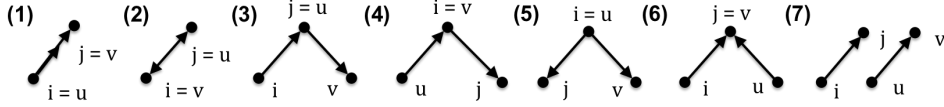


FIG 3. Seven possible configurations of two edges $(i, j), (u, v)$ randomly chosen, with replacement, from a directed graph: (1) two edges degenerate into one $((i, j) = (u, v))$; (2) two opposite edges (the two end nodes point to each other); (3)-(6) four different configurations with the two edges sharing one node; (7) two edges without any node sharing.

4. Analytic type I error control. Given the max-type edge-count scan statistic, the next question is how large does it need to be to constitute sufficient evidence against the null hypothesis of homogeneity. In other words, we are concerned with the tail probability of the scan statistics under H_0 :

$$\begin{aligned} \mathbf{P}\left(\max_{n_0 \leq t \leq n_1} M(t) > b\right) &= 1 - \mathbf{P}\left(\max_{n_0 \leq t \leq n_1} Z_w(t) < b\right) \mathbf{P}\left(\max_{n_0 \leq t \leq n_1} |Z_{\text{diff}}(t)| < b\right) \quad (5) \\ &= 1 - \left(1 - \mathbf{P}\left(\max_{n_0 \leq t \leq n_1} Z_w(t) > b\right)\right) \left(1 - \mathbf{P}\left(\max_{n_0 \leq t \leq n_1} |Z_{\text{diff}}(t)| > b\right)\right). \quad (6) \end{aligned}$$

For a small n , the probability (5) can be obtained by doing permutation directly. However, when n is large, doing permutation could be very time-consuming. Hence, we derive analytic formulas to approximate the probability based on the asymptotic properties of the scan statistic. We first work out the limiting distributions of $\{Z_w([nu])^1 : 0 < u < 1\}$ and $\{Z_{\text{diff}}([nu]) : 0 < u < 1\}$ jointly. On a directed graph, we use $e = (e_-, e_+)$ to denote an edge connected from e_- to e_+ . Let

$$A_e = G_{e_-} \cup G_{e_+},$$

be the subgraph in G that connect to either node e_- or node e_+ , and

$$B_e = \cup_{e^* \in A_e} A_{e^*},$$

be the subgraph in G that connect to any edge in A_e . In the following, we write $a_n = O(b_n)$ when a_n has the same order as b_n , and write $a_n = o(b_n)$ when a_n has order smaller than b_n .

THEOREM 3. *If $|G| = O(n^\beta)$, $1 \leq \beta < 1.5$, $\sum_{e \in G} |A_e| |B_e| = o(n^{1.5\beta})$, $\sum_{e \in G} |A_e|^2 = o(n^{\beta+0.5})$, and $\sum_{i=1}^n |D_i|^2 - k^2 n = O(\sum_{i=1}^n |D_i|)$, as $n \rightarrow \infty$, $\{Z_w([nu]) : 0 < u < 1\}$ and $\{Z_{\text{diff}}([nu]) : 0 < u < 1\}$ converge to independent Gaussian processes in finite dimensional distributions.*

Here, we do not consider $\beta < 1$ as that means the majority of points are not connected and such a graph does not fully use the information among the observations. The proof for the theorem is in the supplement.

¹For a scalar x , we use $[x]$ to denote the largest integer no greater than x

Based on Theorem 3, we have

$$\mathbf{P}\left(\max_{n_0 \leq t \leq n_1} Z_w(t) > b\right) \approx b\phi(b) \int_{n_0}^{n_1} C_w(t) \nu(\sqrt{2b^2 C_w(t)}) dt \quad (7)$$

$$\mathbf{P}\left(\max_{n_0 \leq t \leq n_1} |Z_{\text{diff}}(t)| > b\right) \approx 2b\phi(b) \int_{n_0}^{n_1} C_{\text{diff}}(t) \nu(\sqrt{2b^2 C_{\text{diff}}(t)}) dt \quad (8)$$

where the function $\nu(\cdot)$ can be estimated numerically as

$$\nu(x) \approx \frac{(2/x)(\Phi(x/2) - 0.5)}{(x/2)\Phi(x/2) + \phi(x/2)}$$

with $\phi(\cdot)$ and $\Phi(\cdot)$ being the probability density function and cumulative distribution function of a standard normal distribution, respectively, and

$$C_j(t) = \lim_{s \nearrow t} \frac{\partial \rho_j(s, t)}{\partial s} \quad \text{with} \quad \rho_j(s, t) = \text{Cov}(Z_j(s), Z_j(t)), \quad j = w, \text{ or diff.}$$

The explicit expressions for $C_w(t)$ and $C_{\text{diff}}(t)$ can be derived and simplified to be

$$C_w(t) = \frac{n(n-1)(2t^2/n - 2t + 1)}{2t(n-t)(t^2 - nt + n - 1)}, \quad \text{and} \quad C_{\text{diff}}(t) = \frac{n}{2t(n-t)}.$$

The details are in the supplement.

TABLE 4
Critical values for the scan statistics $\max_{n_0 \leq t \leq n_1} M(t)$ based on 3-NN's graph at $\alpha = 0.05$.

	$n_0 = 100$	$n_0 = 75$	$n_0 = 50$	$n_0 = 25$
A1	3.23	3.27	3.32	3.38

Distributions and dimensions		Critical Values							
		$n_0 = 100$		$n_0 = 75$		$n_0 = 50$		$n_0 = 25$	
		A2	Per	A2	Per	A2	Per	A2	Per
Multivariate Gaussian	$d = 10$	3.26	3.26	3.31	3.35	3.39	3.43	3.52	3.60
	$d = 100$	3.29	3.29	3.36	3.40	3.45	3.52	3.62	3.78
	$d = 1,000$	3.31	3.31	3.40	3.42	3.51	3.60	3.70	3.94
Multivariate t_5	$d = 10$	3.26	3.26	3.32	3.34	3.39	3.44	3.51	3.60
	$d = 100$	3.30	3.30	3.35	3.39	3.44	3.51	3.60	3.79
	$d = 1,000$	3.30	3.30	3.46	3.54	3.59	3.75	3.80	4.27
Multivariate log-normal	$d = 10$	3.27	3.28	3.32	3.33	3.40	3.41	3.52	3.58
	$d = 100$	3.28	3.28	3.35	3.37	3.43	3.48	3.58	3.70
	$d = 1,000$	3.36	3.41	3.45	3.58	3.58	3.81	3.72	4.07

Table 4 shows the performance of the asymptotic p -value approximation of the max-type edge-count scan statistic (5) under different settings. We examine three different underlying distributions (multivariate Gaussian, multivariate t_5 , and multivariate log-normal distributions) with different data dimensions ($d = 10, 100, 1000$). In Table 4, column **Per** is the critical value obtained from doing 10,000 permutations. This can be deemed as close to the true critical value. **A1**

presents the critical values given by substituting (6) by (7) and (8). When n_0 is small, formula (5) is not that close to the critical values obtained through permutations. This is due to the fact that $Z_w(t)$ and $Z_{\text{diff}}(t)$ converge to the normal distributions slowly when t is close to 1 or n . We perform skewness correction to improve the p -value approximations. Column **A2** lists the skewness corrected critical values. The skewness correction protocol is briefly discussed below.

Since the converge of $Z_w(t)$ and $Z_{\text{diff}}(t)$ to the limiting distribution depends on t , we adopt a similar treatment in (Chen and Zhang, 2015; Chu and Chen, 2019) that the skewness correction terms depend on t . The tail probability after skewness correction, is approximated by (with $j = w, \text{diff}$)

$$\mathbf{P}\left(\max_{n_0 \leq t \leq n_1} Z_j(t) > b\right) \approx b\phi(b) \int_{n_0}^{n_1} S_j(t) C_j(t) \nu(\sqrt{2b^2 C_j(t)}) dt \quad (9)$$

where the skewness correction term

$$S_j(t) = \frac{\exp\left(\frac{1}{2}(b - \hat{\theta}_{b,j}(t))^2 + \frac{1}{6}\gamma_j(t)\hat{\theta}_{b,j}^3(t)\right)}{\sqrt{1 + \gamma_j(t)\hat{\theta}_{b,j}(t)}}$$

with $\gamma_j(t) = \mathbf{E}(Z_j^3(t))$ and $\hat{\theta}_{b,j}(t) = (-1 + \sqrt{1 + 2b\gamma_j(t)})/\gamma_j(t)$.

Perfroming skewness correction requires the computation of the third moments of the edge-count test statistics. That is, $\mathbf{E}(Z_w^3(t))$ and $\mathbf{E}(Z_{\text{diff}}^3(t))$. Since those test statistics are linear combinations of $R_{G,1}(t)$ and $R_{G,2}(t)$, all we need is to compute $\mathbf{E}(R_{G,1}^3(t))$ and $\mathbf{E}(R_{G,2}^3(t))$. The computation involves the analysis of the configurations of each set of three edges on the graph. For an undirected graph, there are 8 possible such configurations as discussed in (Chen and Zhang, 2015). However, for a directed graph, there are 24 possible configurations for a set of three edges (Figure 4). We derive analytic formulas to the numbers of those configurations for the directed k -NN graphs, and they are listed in the supplement.

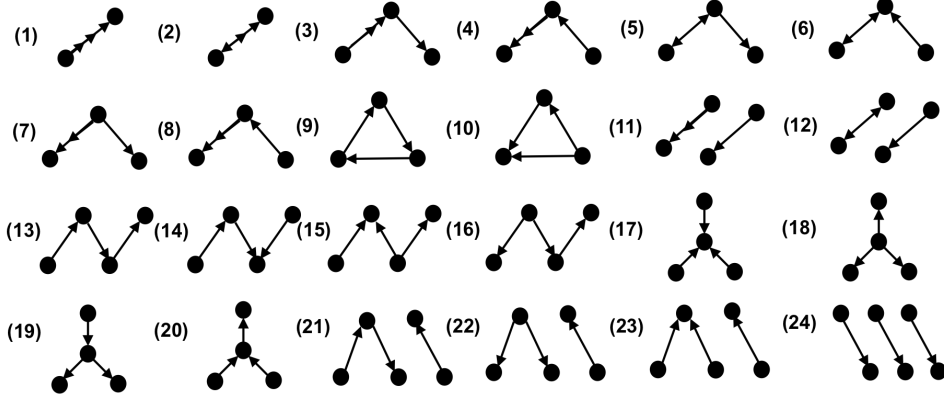


FIG 4. Twenty-four possible configurations of three edges randomly chosen, with replacement, from a directed graph.

5. Conclusion. We propose a new non-parametric framework for change-point analysis using approximation k -NN information. There are fast algorithms available for obtaining the approximate k -NN graph and the time complexity can easily be achieved at $O(dn \log n)$. In constructing the test statistic, we take into account a pattern caused by the curse of dimensionality. As a result, the new test can detect various types of changes for data in moderate to high dimensions, such as change in mean and/or variance, and change in the covariance matrix. There is no distributional assumption on the data. The distribution could be heavy-tailed and/or skewed, the dimension of the data could be much higher than the number of observations, and the change could be global or in a sparse/dense subset of coordinates. We also derive analytic formulas to compute the test statistic and to approximate the p -value, so that the entire algorithm is of time complexity $O(dn \log n)$. Our method is so far the fastest change-point detection method available for detecting various types of changes in long sequences of moderate- to high-dimensional data with proper control on false discoveries.

The proposed framework can easily be extended to non-Euclidean data – as long as a similarity measure can be defined on the sample space, an (approximate) k -NN graph can be constructed and our test can be applied. In this work, we focus on the single change-point alternative. In practice, a sequence could have more than one change-point. Our method can also be extended to deal with multiple change-points by incorporating binary segmentation or wild binary segmentation techniques (Fryzlewicz, 2020; Fryzlewicz et al., 2014; Vostrikova, 1981).

References.

- BEYGELZIMER, A., KAKADET, S., LANGFORD, J., ARYA, S., MOUNT, D. and LI, S. (2019). Fast Nearest Neighbor Search Algorithms and Applications R package FNN: kd-tree fast k-nearest neighbor search algorithms.
- CARLSTEIN, E. G., MÜLLER, H.-G. and SIEGMUND, D. (1994). Change-point problems. IMS.
- CHAN, H. P., WALTHER, G. et al. (2015). Optimal detection of multi-sample aligned sparse signals. *The Annals of Statistics* **43** 1865–1895.
- CHEN, H., CHEN, S. and DENG, X. (2019). A Universal Nonparametric Event Detection Framework for Neuropixels Data. *bioRxiv*.
- CHEN, J. and GUPTA, A. K. (2011). *Parametric statistical change point analysis: with applications to genetics, medicine, and finance*. Springer Science & Business Media.
- CHEN, H. and ZHANG, N. (2015). Graph-based change-point detection. *The Annals of Statistics* **43** 139–176.
- CHU, L. and CHEN, H. (2019). Asymptotic distribution-free change-point detection for multivariate and non-euclidean data. *The Annals of Statistics* **47** 382–414.
- EAGLE, N., PENTLAND, A. S. and LAZER, D. (2009). Inferring friendship network structure by using mobile phone data. *Proceedings of the national academy of sciences* **106** 15274–15278.
- FRYZLEWICZ, P. (2020). Detecting possibly frequent change-points: Wild Binary Segmentation 2 and steepest-drop model selection. *Journal of the Korean Statistical Society* 1–44.
- FRYZLEWICZ, P. et al. (2014). Wild binary segmentation for multiple change-point detection. *The Annals of Statistics* **42** 2243–2281.
- HARCHAOUI, Z., MOULINES, E. and BACH, F. R. (2009). Kernel change-point analysis. In *Advances in neural information processing systems* 609–616.
- HEARD, N. A., WESTON, D. J., PLATANIOTI, K., HAND, D. J. et al. (2010). Bayesian anomaly detection methods for social networks. *The Annals of Applied Statistics* **4** 645–662.
- JAMES, B., JAMES, K. L. and SIEGMUND, D. (1992). Asymptotic approximations for likelihood ratio tests and confidence regions for a change-point in the mean of a multivariate normal distribution. *Statistica Sinica* 69–90.

- KOSSINETIS, G. and WATTS, D. J. (2006). Empirical analysis of an evolving social network. *science* **311** 88–90.
- LI, Z., LI, P., KRISHNAN, A. and LIU, J. (2011). Large-scale dynamic gene regulatory network inference combining differential equation models with local dynamic Bayesian network analysis. *Bioinformatics* **27** 2686–2691.
- LU, T., LIANG, H., LI, H. and WU, H. (2011). High-dimensional ODEs coupled with mixed-effects modeling techniques for dynamic gene regulatory network identification. *Journal of the American Statistical Association* **106** 1242–1258.
- MATTESON, D. S. and JAMES, N. A. (2014). A nonparametric approach for multiple change point analysis of multivariate data. *Journal of the American Statistical Association* **109** 334–345.
- SIEGMUND, D., YAKIR, B. and ZHANG, N. R. (2011). Detecting simultaneous variant intervals in aligned sequences. *The Annals of Applied Statistics* 645–668.
- SRIVASTAVA, M. and WORSLEY, K. J. (1986). Likelihood ratio tests for a change in the multivariate normal mean. *Journal of the American Statistical Association* **81** 199–204.
- STRINGER, C., PACHITARIU, M., STEINMETZ, N., REDDY, C. B., CARANDINI, M. and HARRIS, K. D. (2019). Spontaneous behaviors drive multidimensional, brainwide activity. *Science* **364** eaav7893.
- VOSTRIKOVA, L. Y. (1981). Detecting disorder in multidimensional random processes. **259** 270–274.
- WANG, T. and SAMWORTH, R. J. (2018). High dimensional change point estimation via sparse projection. *Journal of the Royal Statistical Society: Series B (Statistical Methodology)* **80** 57–83.
- WANG, H., TANG, M., PARK, Y. and PRIEBE, C. E. (2013). Locality statistics for anomaly detection in time series of graphs. *IEEE Transactions on Signal Processing* **62** 703–717.
- XIE, Y. and SIEGMUND, D. (2013). Sequential multi-sensor change-point detection. In *2013 Information Theory and Applications Workshop (ITA)* 1–20. IEEE.
- ZHANG, N. R., SIEGMUND, D. O., JI, H. and LI, J. Z. (2010). Detecting simultaneous changepoints in multiple sequences. *Biometrika* **97** 631–645.